

Safety-Critical Containment Control for Multi-Agent Systems With Communication Delays

Zilong Song , Student Member, IEEE, Zheyuan Wu , Student Member, IEEE, and Haocai Huang , Member, IEEE

Abstract—Recently, the containment control for multi-agent systems (MASs) with communication delays has been studied. However, in these existing results, the assumptions for delays are too strong, leading to deviations from reality; moreover, safety is rarely considered, especially under a surging number of collision threats and the state constraint. In this work, we focus on the containment control for MASs with nonuniform time-varying communication delays; the formation configuration is extended to a dynamic one with time-varying velocity, and the model of agents is extended to the Euler–Lagrange (EL) model with uncertainty. We present sufficient conditions for containment control in the above case by utilizing the Lyapunov–Krasovskii function and the linear matrix inequalities (LMIs). Moreover, we propose a robust control barrier function (CBF)-based obstacle avoidance approach that ensures MAS safety through optimal control, thus better synthesizing the conflict between safety and the original control goals. In addition, considering that model uncertainty can adversely affect CBFs, we propose an observer with a quantified error to provide CBFs with robustness against uncertainty. Finally, simulation results demonstrate the validity of the proposed method.

Index Terms—Containment control with communication delays, control barrier functions, optimal control, safety-critical control.

I. INTRODUCTION

COORDINATION control for multi-agent systems (MASs) has received widespread attention in recent years [1]. In some complex scenarios, there may exist more than one leader, and followers are expected to enter the area spanned by several leaders. This is termed containment control [2] and is widely used in unmanned aerial vehicles [3], spacecraft [4], and underwater vehicles [5]. Moreover, safety is a major concern in dynamic systems [6], and it is challenging to deal with potential conflicts between safety and original control objectives. The safety-critical control method [7], in which system safety is prioritized over initial control missions, has become a powerful

Manuscript received 14 January 2024; revised 11 April 2024; accepted 13 May 2024. Date of publication 15 May 2024; date of current version 16 August 2024. This work was supported in part by the Project of the Donghai Laboratory under Grant DH-2022ZY0004, in part by the National Natural Science Foundation of China under Grant 52017293, and in part by the National Key Research and Development Program of China under Grant 2017YFC0306100. Recommended for acceptance by Prof. Eirini Eleni Tsipoulopoulou. (*Corresponding author: Haocai Huang*)

Zilong Song and Zheyuan Wu are with the Ocean College, Zhejiang University, Zhoushan 316021, China (e-mail: zilong_song@zju.edu.cn).

Haocai Huang is with the Ocean College, Zhejiang University, Zhoushan 316021, China, also with the Qingdao National Laboratory for Marine Science and Technology, Qingdao 266061, China, also with the Hainan Institute of Zhejiang University, Hainan 572025, China, and also with the Donghai Laboratory, Zhoushan 316021, China (e-mail: hchuang@zju.edu.cn).

Digital Object Identifier 10.1109/TNSE.2024.3401592

tool for guaranteeing system safety. In this context, control barrier functions [8], as safety filters for nominal controllers, provide provable safety via optimization and are widely used in safety-critical controls [9].

Containment control, as a particular form of coordination control, has advanced in several directions based on extensive fundamental research. The models of the agents have been developed from first-order [10] to Euler–Lagrange [11] and high-order models [12], and model uncertainty is addressed by observers [13] and neural networks [14]. Meanwhile, there are many results on prescribed performance [15], event-triggered [16], fault-tolerant [17], and finite-time containment control [18], and some other concerns, such as input saturation [19], underactuated [20], and switching topologies [21], have been well studied in existing work. However, in addition to the above concerns, communication delays, which are inevitable in practical situations [22], [23], need to be considered.

Since communication delays can affect performance and even render the system unstable [24], [25], much work has been focused on containment control with communication delays. In order to combat the adverse effects of delays on the system, an appropriate control law is required and, most importantly, the parameters in control law need to fulfill certain conditions. We note that deriving these conditions is the key to solving the problem, which is the focus of most existing work [26], [27]. Lyapunov–Krasovskii functions have become a powerful tool for deriving the sufficient conditions for parameters [28], [29]. Moreover, delays in more general forms such as time-varying delays [30] and nonuniform delays [31] mean a wider range of application scenarios; nevertheless, more effort is required since the difficulty of deriving the conditions increases with the complexity of the delays. In the latest results, [31] studied the containment control for double-integrator agents with constant nonuniform communication delays, in which the leaders are assumed to move with a constant velocity. The time-varying nonuniform delay, as a more general case, was studied in [24] at the cost that multiple leaders can only be stationary, i.e., the control law is confined to a static formation configuration. Note that as the most general case for formation configuration, the containment control for dynamic formations with time-varying velocity was studied in the latest work [32], [33]; nevertheless, these results restrict delays to be uniform, and the agent's dynamics were limited to linear systems. We see that among the above topics, the time-varying nonuniform delays and dynamic formations with time-varying velocities have greater potential for application. However, to the best of our knowledge, few

studies have achieved both of these goals simultaneously in the context of containment control.

It is worth noting that in addition to communication delays, safety guarantees are another main concern in real system [34]. Specifically, safety guarantee means that all agents should be able to avoid obstacles in the environment. We note that this safety requirement is particularly acute in containment control, since the desired position of agents is determined collectively by their neighbors, which makes it difficult to plan safe paths in advance. Artificial potential fields (APFs) that directly add potential function terms to the control law are widely used in obstacle avoidance [35], [36]. However, when collision threat increases, they cannot properly handle the conflict between safety and the original control goals [37]. Moreover, the state constraints, typically position or velocity constraints caused by workspace limitations, cannot be well addressed by APFs. The safety-critical control, which can synthesize these potential conflicts and state constraints and place safety in the highest priority [38], [39], has become a popular topic in safety assurance. Recently, the control barrier functions (CBFs) have emerged as powerful tools for safety-critical control [40]. They first define a safety set and then present constraints that make this safety set forward invariant [41]; thus, safety can be ensured by modifying the nominal control law to meet these constraints. In this context, safety assurance is transformed into an optimization problem with safety constraints and state constraints (if any). Due to its reliability and real-time performance, CBF-based safety-critical control has gradually been used for obstacle avoidance in many robotic systems, such as manipulators [42], autonomous surface vehicles [43], and quadrotors [44].

However, one obvious barrier to wider application of CBFs is that the construction of CBFs relies on an accurate model. The model uncertainty in CBFs may lead to a wrong safety constraint thus the optimized control input cannot guarantee system safety. Several existing works account for this problem, a robust CBF is proposed in [45], which considers the worst case caused by the uncertainty and uses the boundary of the uncertainty to construct robust safety conditions; an input-to-state safety CBF is presented in [46], which is an extension of input-to-state stability (ISS) theory and can be used to ensure the safety of the systems with input disturbances; a Gaussian process-based CBF is proposed in [47], which uses Gaussian process (GP) to predict the model uncertainty in the CBF. The above studies have improved the CBF's ability to deal with uncertainty, but there are also some drawbacks. Specifically, the robust CBF in [45] provides the strictest condition by using the uncertainty boundary, which leads to conservative control inputs and poor tracking performance [48]. The input-to-state safety CBF can only account for the input disturbance and lacks generalization as the uncertainty can also arise from inaccurate parameters [49] and external disturbances. The GP-based CBF has expensive computational burden [50] since the GP prediction is a data-driven method and its basic complexity is $\mathcal{O}(n^3)$ [51]. Therefore, there is a need for a generic method that can provide a better trade-off between safety and performance while having a lower computational cost.

Motivated by the above results, containment control under communication delays in the most general case is studied for the first time. A robust CBF-based obstacle avoidance method is proposed for containment control to guarantee MASs safety, where the robustness is given by an observer with quantified error. The three main contributions of this study are as follows.

1) As the most general case, the containment control for dynamic MASs moving with time-varying velocity subject to time-varying nonuniform communication delays remains an open challenge. This is the first study to provide the sufficient conditions for containment control in the above case, which is achieved by constructing a Lyapunov–Krasovskii function and developing stability conditions in the form of LMIs. Moreover, the model of agents is extended to the Euler–Lagrange model with uncertainty for a wider range of applications. We remove the restriction in existing work that delays can only be uniform in dynamic formation configuration, and the results in [24], [32] can be considered as special cases of this work.

2) The CBFs-based safety-critical control approach is combined with containment control for obstacle avoidance, in which CBFs provide safety conditions, and then obstacle avoidance can be achieved through the optimal control with multiple constraints. Compared to existing results using APFs [35], [36], this method can better synthesize the conflicts between safety and control performance via the optimization approach, even when agents are subjected to moving obstacles, state constraints (position and velocity), and a surging number of collision threats.

3) An observer-based robust CBF is proposed to address the impact of model uncertainty on safety guarantees, i.e., obstacle avoidance. An observer is designed to estimate the uncertainty emerging in the CBF with a quantified estimation error; the estimation is then used to recover the CBF, and an additional term is introduced to provide robustness against the quantified error. Compared to the data-driven CBFs [47] and CBFs that only consider the worst case [45], this work provides a better trade-off between safety and control performance at lower computational cost.

The rest of this paper is organized as follows. Section II presents the preliminaries. The nominal containment control law is designed in Section III. The safety-critical containment control law is provided in Section IV. Simulation results are provided in Section V. Section VI concludes the article.

Notation: \otimes refers to the Kronecker product, $f_1 \circ f_2$ refers to the composition of functions f_1 and f_2 , and for $a_i \in \mathbb{R}^d$, $\text{col}(a_1, \dots, a_n) = [a_1^T, \dots, a_n^T]^T \in \mathbb{R}^{nd}$.

II. PRELIMINARIES

A. Dynamic Model

We consider a multi-agent system (MAS) with m followers and n virtual leaders. The dynamics of followers are described by Euler–Lagrange (EL) model

$$M_i(q_i)\ddot{q}_i + C_i(q_i, \dot{q}_i)\dot{q}_i + G_i(q_i) = \tau_i, \quad (1)$$

where $i \in \{1, \dots, m\}$ denotes the i -th follower, q_i , \dot{q}_i , and $\ddot{q}_i \in \mathbb{R}^d$ represent the position, velocity, and acceleration, respectively, and d is the degree of freedom. $M_i(q_i)$ denotes the inertia matrix, $C_i(q_i, \dot{q}_i)$ denotes the unknown Coriolis and centrifugal term, $G_i(q_i)$ is the unknown gravitational term, and $\tau_i \in \mathbb{R}^d$ stands for the control input.

Remark 1: The EL model (1) can capture the dynamics of many systems and is widely used in robotic systems, such as quadrotors [52], wheeled-mobile robots [53], autonomous underwater vehicles [54], and manipulators [55].

In addition, the EL system has the following properties [56]:

Property 1: The matrix $\dot{M}_i - 2C_i$ is skew symmetric. Therefore, $a^T(\dot{M}_i - 2C_i)a = 0$ for any $a \in \mathbb{R}^d$.

Property 2: $\exists \bar{m} > 0$, $\underline{m} > 0$ such that $\underline{m}I_d < M_i < \bar{m}I_d$, and C_i and G_i are bounded with bounded q_i and \dot{q}_i .

Property 3: The dynamics in system (1) can be linearly parameterized; i.e., for any $x, y \in \mathbb{R}^d$, we have

$$M_i(q_i)x + C_i(q_i, \dot{q}_i)y + G_i(q_i) = Y_i(q_i, \dot{q}_i, x, y)\theta_i \quad (2)$$

where $Y_i(q_i, \dot{q}_i, x, y) \in \mathbb{R}^{d \times k}$ is a regressor matrix and $\theta_i \in \mathbb{R}^k$ is an unknown constant parameter vector, with k being the number of regression functions for each freedom degree in the regression matrix.

B. Graph Theory

For a graph $\mathcal{G} = (\mathcal{V}, \mathcal{E})$, $\mathcal{V} = \{b_1, \dots, b_i, \dots, b_n\}$ represents the node set with b_i corresponding to the i -th agent, and $\mathcal{E} \subseteq \mathcal{V} \times \mathcal{V}$ represents the edge set. The adjacency matrix is denoted as $A = [a_{ik}] \in \mathbb{R}^{n \times n}$, where $a_{ik} = 1$ if $(b_k, b_i) \in \mathcal{E}$, which means that the information of the k -th agent is reachable for the i -th agent; otherwise, $a_{ik} = 0$. The Laplacian matrix is defined by $L = [l_{ik}] \in \mathbb{R}^{n \times n}$, where $l_{ii} = \sum_{k=1, k \neq i}^n a_{ik}$, $l_{ik} = -a_{ik}$, and $i \neq k$.

In this paper, graph \mathcal{G}_A depicts the communication between all agents whose Laplacian matrix is defined as

$$L_A = \begin{pmatrix} L_1 & L_2 \\ \mathbf{0}_{n \times m} & \mathbf{0}_{n \times n} \end{pmatrix}, \quad (3)$$

where $L_1 \in \mathbb{R}^{m \times m}$ and $L_2 \in \mathbb{R}^{m \times n}$ reflect the interactions among followers and between leaders and followers, respectively.

In order to address the nonuniform communication delays, we suppose that there are X_1 types of delays among followers and X_2 types of delays between leaders and followers. The total number of types is X and satisfying $X \leq X_1 + X_2$. Then, we can define the delay sets as $D_1 = \{T_a(t) : a = 1, \dots, X_1\}$ and $D_2 = \{T_a(t) : a = X_1 + 1, \dots, X_1 + X_2\}$. For further analysis, we consider $\mathcal{G}_{A,a}$ as a subgraph of \mathcal{G}_A , in which the delay among agents is $T_a(t)$, and the corresponding Laplacian matrix of $\mathcal{G}_{A,a}$ can be defined by

$$L_{A,a} = \begin{pmatrix} L_{1,a} & L_{2,a} \\ \mathbf{0}_{n \times m} & \mathbf{0}_{n \times n} \end{pmatrix}, \quad (4)$$

In this case, we have $\sum_{a=1}^X L_{1,a} = L_1$ and $\sum_{a=1}^X L_{2,a} = L_2$. [24]

C. Assumptions and Control Objective

Assumption 1: For each follower, there exists at least one virtual leader that has a directed path to that follower.

Assumption 2: The communication delay $T_a(t)$ is bounded, differentiable, and satisfies $0 < T_a(t) < \varphi$, $|\dot{T}_a(t)| \leq \gamma \leq 1$, where φ and γ are constants.

The control objectives can be described as follows.

Containment control: Drive followers to enter a convex hull spanned by leaders despite communication delays, i.e., [57]

$$\lim_{t \rightarrow \infty} q_F = -(L_1^{-1} L_2 \otimes I_d) q_L \quad (5)$$

where $q_F = \text{col}(q_1, \dots, q_m)$ and $q_L = \text{col}(q_{m+1}, \dots, q_{m+n})$.

Safety guarantee: Ensure that all agents are able to avoid stationary and moving obstacles.

III. CONTAINMENT CONTROL UNDER TIME-VARYING COMMUNICATION DELAYS

A. Nominal Control Law Design

In the context of distributed control, we propose an observer to estimate the desired velocity.

$$\begin{aligned} \dot{\hat{v}}_i &= -\lambda \sum_{j=1}^m a_{ij} (\hat{v}_i(t_{ij}) - \hat{v}_j(t_{ij})) \\ &\quad - \lambda \sum_{k=m+1}^{m+n} a_{ik} (\hat{v}_i(t_{ik}) - \dot{q}_k(t_{ik})) \end{aligned} \quad (6)$$

where $t_{ij} = t - T_{ij}(t)$, with $T_{ij}(t) \in D_1$ being the time-varying communication delay between the i -th and j -th followers, $t_{ik} = t - T_{ik}(t)$, with $T_{ik}(t) \in D_2$ being the time-varying delay between the i -th follower and the k -th leader, $\lambda > 0$, \hat{v}_i is the estimate of the desired velocity for the i -th follower, and \dot{q}_k denotes the velocity of the k -th leader.

Next, we introduce two auxiliary variables

$$\dot{\zeta} = \hat{v}_i - \sigma \sum_{j=1}^{m+n} a_{ij} (q_i(t_{ij}) - q_j(t_{ij})), \quad (7)$$

$$\vartheta_i = \dot{q}_i - \dot{\zeta} = \dot{q}_i - \hat{v}_i + \sigma \sum_{j=1}^{m+n} a_{ij} (q_i(t_{ij}) - q_j(t_{ij})), \quad (8)$$

where $\sigma > 0$. Meanwhile, according to Property 3 of the EL system, we have

$$M_i(q_i)\ddot{\zeta}_i + C_i(q_i, \dot{q}_i)\dot{\zeta}_i + G_i(q_i) = Y_i(q_i, \dot{q}_i, \dot{\zeta}_i)\theta_i, \quad (9)$$

where $\ddot{\zeta}_i$ in the regressor matrix Y_i can be computed as

$$\begin{aligned} \ddot{\zeta} &= \dot{\hat{v}}_i - \sigma \sum_{j=1}^{m+n} a_{ij} (\dot{q}_i(t_{ij}) - \dot{q}_j(t_{ij})) \\ &= -\lambda \sum_{j=1}^m a_{ij} (\hat{v}_i(t_{ij}) - \hat{v}_j(t_{ij})) - \lambda \sum_{k=m+1}^{m+n} a_{ik} (\hat{v}_i(t_{ik}) - \dot{q}_k(t_{ik})) \\ &\quad - \sigma \sum_{j=1}^{m+n} a_{ij} (\dot{q}_i(t_{ij}) - \dot{q}_j(t_{ij})) \end{aligned} \quad (10)$$

Then, the nominal containment control law is designed

$$\bar{\tau}_i = -K_i \vartheta_i + Y_i \hat{\theta}_i, \quad (11)$$

where $K_i > 0$ and $\hat{\theta}_i$ is the estimate of unknown θ_i , whose adaptive law is designed as

$$\dot{\hat{\theta}}_i = -\Xi_i Y_i^T (q_i, \dot{q}_i, \dot{\zeta}_i, \ddot{\zeta}_i) \vartheta_i, \quad (12)$$

where $\Xi_i > 0$ is the gain matrix.

We note that $\bar{\tau}_i$ is the nominal control law, which is optimized through a quadratic program with safety constraints in Section IV to achieve obstacle avoidance.

Remark 2: We note that the delays considered in this work are nonuniform and time-varying; meanwhile, the formation configuration is dynamic with time-varying velocity. Thus, we remove the restriction in existing studies that delays can only be uniform in dynamic formation configuration. Moreover, the agent models are extended to EL systems with uncertainties for broader applications.

B. Stability Analysis

Theorem 1: Consider the MAS (1) under nonuniform time-varying communication delays, with control law (6), (7), (8), (11), and (12), the containment control can be achieved if the parameters in the control law are designed such that

$$\bar{\Theta} < 0, \bar{\Pi} < 0 \quad (13)$$

where $\bar{\Theta}$ and $\bar{\Pi}$ are defined in (31) and (33), respectively.

Proof: To facilitate further processing, we first denote ϑ_F , ζ_F , q_F , and θ_F as the column stack vectors framed by $(\bullet)_F = [(\bullet)_1^T, \dots, (\bullet)_m^T]^T$, and M_F , C_F , K_F , Ξ_F , and Y_F are block diagonal matrices framed by $(\bullet)_F = \text{diag}[(\bullet)_1, \dots, (\bullet)_m]$.

Then, substituting (11) into (1) and writing the result in a compact form, we have

$$M_F \dot{\vartheta}_F + C_F \vartheta_F = -K_F \vartheta_F - Y_F \tilde{\theta}_F, \quad (14)$$

where $\tilde{\theta}_F = \theta_F - \hat{\theta}_F$. Then, we consider the Lyapunov function candidate as follows

$$V_* = \frac{1}{2} (\vartheta_F^T M_F \vartheta_F + \tilde{\theta}_F^T \Xi_F^{-1} \tilde{\theta}_F), \quad (15)$$

The derivative of (15) can be calculated as

$$\begin{aligned} \dot{V}_* &= \vartheta_F^T M_F \dot{\vartheta}_F + \frac{1}{2} \vartheta_F^T \dot{M}_F \vartheta_F - \tilde{\theta}_F^T \Xi_F^{-1} \dot{\tilde{\theta}}_F \\ &= \frac{1}{2} \vartheta_F^T (M_F - 2C_F) \vartheta_F - \vartheta_F^T K_F \vartheta_F \\ &= -\vartheta_F^T K_F \vartheta_F \end{aligned} \quad (16)$$

where the second equation is derived from (12) and (14), and the last equation follows from $\vartheta_F^T (M_F - 2C_F) \vartheta_F = 0$ according to Property 1.

Note that $V_* > 0$ if $\vartheta_F \neq 0, \tilde{\theta}_F \neq 0$, and $\dot{V}_* \leq 0$ since K_F is positive definite; then, we can conclude that $\lim_{t \rightarrow \infty} V_*$ is finite and that ϑ_F and $\tilde{\theta}_F$ are bounded. According to (14) and Property 2, $\dot{\vartheta}_F$ is bounded; then we can get $\ddot{V}_* = -2\vartheta_F^T K_F \dot{\vartheta}_F$ is bounded. Based on Barbalat's Lemma, we get $\lim_{t \rightarrow \infty} \dot{V}_* = 0$, and thus, $\lim_{t \rightarrow \infty} \vartheta_F = 0$.

Then, the position error and velocity error in containment control can be expressed as

$$\dot{e}_F = q_F + (L_1^{-1} L_2 \otimes I_d) q_L, \quad (17)$$

$$\dot{\nu}_F = \hat{\nu}_F + (L_1^{-1} L_2 \otimes I_d) \dot{q}_L, \quad (18)$$

where $e_F = \text{col}(e_1, \dots, e_m)$, $\hat{\nu}_F = \text{col}(\hat{\nu}_1, \dots, \hat{\nu}_m)$. Meanwhile, (8) and (6) can be rewritten as

$$\begin{aligned} \vartheta_F &= \dot{q}_F - \hat{\nu}_F + \sigma \sum_{a=1}^X (L_{1,a} \otimes I_d) q_F(t_a) \\ &\quad + \sigma \sum_{a=1}^X (L_{2,a} \otimes I_d) q_L(t_a) \end{aligned} \quad (19)$$

$$\begin{aligned} \dot{\nu}_F &= -\lambda \sum_{a=1}^X (L_{1,a} \otimes I_d) \hat{\nu}_F(t_a) \\ &\quad - \lambda \sum_{a=1}^X (L_{2,a} \otimes I_d) \dot{q}_L(t_a) \end{aligned} \quad (20)$$

where $t_a = t - T_a$, with $T_a \in D_1 \cup D_2$.

Combining (17)–(20) and $\lim_{t \rightarrow \infty} \vartheta_F = 0$, we get

$$\begin{aligned} \dot{e}_F &= \tilde{\nu}_F - \sigma \sum_{a=1}^X (L_{1,a} \otimes I_d) e_F(t_a) \\ \dot{\tilde{\nu}}_F &= -\lambda \sum_{a=1}^X (L_{1,a} \otimes I_d) \tilde{\nu}_F(t_a) + (L_1^{-1} L_2 \otimes I_d) \ddot{q}_L \end{aligned} \quad (21)$$

Note that (21) indicates the error dynamic system; next, we prove the stability of (21). Defining $E(t) = \text{col}(e_F(t), \tilde{\nu}_F(t))$, (21) can be rewritten as

$$\dot{E}(t) = AE(t) + \sum_{a=1}^X B_a E(t_a) + H(t) \quad (22)$$

where $A = \begin{pmatrix} 0 & I_{dm} \\ 0 & 0 \end{pmatrix}$, $B_a = \begin{pmatrix} -\sigma(L_{1,a} \otimes I_d) & 0 \\ 0 & -\lambda(L_{1,a} \otimes I_d) \end{pmatrix}$, and $H(t) = \begin{pmatrix} 0 \\ (L_1^{-1} L_2 \otimes I_d) \ddot{q}_L \end{pmatrix}$.

Then, consider the Lyapunov–Krasovskii function candidate

$$V = \sum_{i=1}^4 V_i \quad (23)$$

with

$$\begin{aligned} V_1 &= X E^T(t) P_1 E(t) \\ V_2 &= \sum_{a=1}^X \int_{t_a}^t E^T(r) P_2 E(r) dr \\ &\quad + X \int_{-\varphi}^0 \int_{t+s}^t \dot{E}^T(r) P_3 \dot{E}(r) dr ds \\ V_3 &= \int_{t-\varphi}^t H^T(r) P_4 H(r) dr + \sum_{a=1}^X \int_{t_a}^t H^T(r) P_5 H(r) dr \\ V_4 &= \varphi \int_{-\varphi}^0 \int_{t+s}^t \dot{H}^T(r) P_6 \dot{H}(r) dr ds \\ &\quad + \frac{\varphi^2}{2} \int_{t-\varphi}^t \int_y^t \int_s^t \dot{H}^T(r) P_7 \dot{H}(r) dr ds dy \end{aligned}$$

where $P_i \in \mathbb{R}^{2dm \times 2dm}$, $i = 1, \dots, 7$ are positive matrices.

Next, we present some necessary lemmas, and then, we calculate the derivatives of V on this basis.

Lemma 1: [58]: For a smooth function $f(t)$, we have

$$\frac{d}{dt} \left(\int_{-a}^0 \int_{t+r}^t f(s) ds dr \right) = af(t) - \int_{t-a}^t f(r) dr \quad (24)$$

Lemma 2: [59]: For a positive matrix A , we have

$$\begin{aligned} & -\frac{(m-n)^2}{2} \int_n^m \int_\theta^m f^T(s) A f(s) ds d\theta \\ & \leq - \left(\int_n^m \int_\theta^m f(s) ds d\theta \right)^T A \left(\int_n^m \int_\theta^m f(s) ds d\theta \right) \end{aligned} \quad (25)$$

Then, the derivatives of V_i can be derived as

$$\begin{aligned} \dot{V}_1 &= X \dot{E}^T(t) P_1 E(t) + X E^T(t) P_1 \dot{E}(t) \\ \dot{V}_2 &\leq E^T(t) X P_2 E(t) - \sum_{a=1}^X (1-\gamma) E^T(t_a) P_2 E(t_a) \\ &+ \varphi X \dot{E}^T(t) P_3 \dot{E}(t) - \sum_{a=1}^X \int_{t_a}^t \dot{E}^T(r) P_3 \dot{E}(r) dr \\ \dot{V}_3 &\leq H^T(t) P_4 H(t) - H^T(t-\varphi) P_4 H(t-\varphi) \\ &+ H^T(t) X P_5 H(t) - \sum_{a=1}^X (1-\gamma) H^T(t_a) P_5 H(t_a) \\ \dot{V}_4 &= \dot{H}^T(t) (\varphi^2 P_6 + \frac{\varphi^4}{4} P_7) \dot{H}(t) - \varphi \int_{t-\varphi}^t \dot{H}^T(r) P_6 \dot{H}(r) dr \\ &- \frac{\varphi^2}{2} \int_{t-\varphi}^t \int_s^t \dot{H}^T(r) P_7 \dot{H}(r) dr ds \\ &\leq \dot{H}^T(t) (\varphi^2 P_6 + \frac{\varphi^4}{4} P_7) \dot{H}(t) - \varphi \int_{t-\varphi}^t \dot{H}^T(r) P_6 \dot{H}(r) dr \\ &- \left(\varphi H^T(t) - \int_{t-\varphi}^t H^T(r) dr \right) P_7 \left(\varphi H(t) - \int_{t-\varphi}^t H(r) dr \right) \end{aligned} \quad (26)$$

Furthermore, according to Lemma 2 in [60], the following inequality holds for any $Q_1, Q_2 \in \mathbb{R}^{2dm \times 2dm}$.

$$\begin{aligned} & - \sum_{a=1}^X \int_{t_a}^t \dot{E}^T(r) P_3 \dot{E}(r) dr \\ & \leq [\bar{E}^T(t) \bar{E}^T(t_d)] \begin{pmatrix} \hat{Q}_1^T + \hat{Q}_1 & -\hat{Q}_1^T + \hat{Q}_2 \\ -\hat{Q}_1 + \hat{Q}_2^T & -\hat{Q}_2^T - \hat{Q}_2 \end{pmatrix} \begin{bmatrix} \bar{E}(t) \\ \bar{E}(t_d) \end{bmatrix} \\ & + \varphi [\bar{E}^T(t) \bar{E}^T(t_d)] \begin{bmatrix} \hat{Q}_1^T \\ \hat{Q}_2^T \end{bmatrix} \hat{P}_3^{-1} [\hat{Q}_1 \hat{Q}_2] \begin{bmatrix} \bar{E}(t) \\ \bar{E}(t_d) \end{bmatrix} \end{aligned} \quad (27)$$

where $\bar{E}(t) = \mathbf{1}_X \otimes E(t)$, $\bar{E}(t_d) = [E^T(t_1) \cdots E^T(t_X)]^T$, $\hat{P}_3 = I_X \otimes P_3$, and $\hat{Q}_i = I_X \otimes Q_i$, $i = 1, 2$.

Meanwhile, based on the Newton–Leibniz formula, we have

$$2\varphi \alpha^T R \left(H(t) - H(t-\varphi) - \int_{t-\varphi}^t \dot{H}(s) ds \right) = 0 \quad (28)$$

where $\alpha = [\dot{H}^T(t) \ H^T(t) \ \bar{H}^T(t_d) \ H^T(t-\varphi) \ \int_{t-\varphi}^t H^T(r) dr \ E^T(t) \ \bar{E}^T(t_d)]^T$ with $\bar{H}(t_d) = [H^T(t_1) \cdots H^T(t_X)]^T$, $R =$

$[R_1^T, \dots, R_7^T]^T$ with $R_3 = R_7 = \mathbf{1}_X \otimes I_{2dm}$ and the remainder $R_i = I_{2dm}$.

Combining (26), (27) and (28), we can obtain

$$\begin{aligned} \dot{V} &\leq \wp^T \left(\Theta + \varphi \begin{bmatrix} \hat{A}^T \\ X \hat{B}_a^T \end{bmatrix} \hat{P}_3 [\hat{A} X \hat{B}_a] + \varphi \begin{bmatrix} \hat{Q}_1^T \\ \hat{Q}_2^T \end{bmatrix} \hat{P}_3^{-1} [\hat{Q}_1 \hat{Q}_2] \right) \wp \\ &+ \alpha^T (\Pi + \varphi^2 R \hat{P}_6^{-1} R^T) \alpha \\ &- \varphi \int_{t-\varphi}^t (\alpha^T R + \dot{H}^T(r) P_6) P_6^{-1} (\alpha^T R + \dot{H}^T(r) P_6)^T dr \end{aligned} \quad (29)$$

where $\wp = [\bar{E}^T(t) \bar{E}^T(t_d)]^T$, $\hat{A} = I_X \otimes A$, $\hat{B}_a = \text{diag}\{B_1, \dots, B_X\}$, and Θ and Π are symmetric matrices defined as

$$\begin{aligned} \Theta_{(1,1)} &= \hat{A}^T \hat{P}_1 + \hat{P}_1 \hat{A} + \hat{P}_2 + \hat{Q}_1^T + \hat{Q}_1, \\ \Theta_{(1,2)} &= X \hat{P}_1 \hat{B}_a - \hat{Q}_1^T + \hat{Q}_2, \quad \Theta_{(2,2)} = (\gamma - 1) \hat{P}_2 - \hat{Q}_2^T - \hat{Q}_2, \\ \Pi_{(1,1)} &= \varphi^2 P_6 + \frac{\varphi^4}{4} P_7, \quad \Pi_{(1,2)} = \varphi R_1, \quad \Pi_{(1,4)} = -\varphi R_1, \\ \Pi_{(2,2)} &= \varphi X P_3 + P_4 + X P_5 - \varphi^2 P_7 + 2\varphi R_2, \quad \Pi_{(2,3)} = \varphi R_3^T, \\ \Pi_{(2,5)} &= \varphi P_7 + \varphi R_5^T, \quad \Pi_{(2,6)} = X P_1 + \varphi X P_3 A + \varphi R_6^T, \\ \Pi_{(2,7)} &= \varphi X P_3 \bar{B}_a + \varphi R_7^T, \quad \Pi_{(3,3)} = (\gamma - 1) \hat{P}_5, \\ \Pi_{(3,4)} &= -\varphi R_3, \quad \Pi_{(4,4)} = -P_4 - 2\varphi R_4, \quad \Pi_{(4,5)} = -\varphi R_5^T, \\ \Pi_{(4,6)} &= -\varphi R_6^T, \quad \Pi_{(4,7)} = -\varphi R_7^T, \quad \Pi_{(5,5)} = -P_7, \end{aligned}$$

with $\hat{P}_i = I_X \otimes P_i$, $\bar{B}_a = [B_1 \cdots B_X]$, and the other terms are zero matrices.

According to Schur's Lemma, we have

$$\begin{aligned} & \Theta + \varphi \begin{bmatrix} \hat{A}^T \\ X \hat{B}_a^T \end{bmatrix} \hat{P}_3 [\hat{A} X \hat{B}_a] \\ & + \varphi \begin{bmatrix} \hat{Q}_1^T \\ \hat{Q}_2^T \end{bmatrix} \hat{P}_3^{-1} [\hat{Q}_1 \hat{Q}_2] < 0 \Leftrightarrow \bar{\Theta} < 0 \end{aligned} \quad (30)$$

where $\bar{\Theta}$ is a symmetric matrix defined as

$$\bar{\Theta} = \begin{pmatrix} \bar{\Theta}_{11} & \bar{\Theta}_{12} \\ \bar{\Theta}_{12}^T & \bar{\Theta}_{22} \end{pmatrix}, \quad (31)$$

with $\bar{\Theta}_{11} = \Theta$, $\bar{\Theta}_{12} = \begin{pmatrix} \hat{A}^T & \hat{Q}_1^T \\ X \hat{B}_a^T & \hat{Q}_2^T \end{pmatrix}$, and $\bar{\Theta}_{22} = -\text{diag}\{\frac{1}{\varphi} \hat{P}_3^{-1}, \frac{1}{\varphi} \hat{P}_3\}$.

In the same way, we know that

$$\Pi + \varphi^2 R \hat{P}_6^{-1} R^T < 0 \Leftrightarrow \bar{\Pi} < 0 \quad (32)$$

where $\bar{\Pi}$ is a symmetric matrix defined as

$$\bar{\Pi} = \begin{pmatrix} \bar{\Pi}_{11} & \bar{\Pi}_{12} \\ \bar{\Pi}_{12}^T & \bar{\Pi}_{22} \end{pmatrix} \quad (33)$$

with $\bar{\Pi}_{11} = \Pi$, $\bar{\Pi}_{12} = \varphi R$, and $\bar{\Pi}_{22} = -P_6$.

Since the last term in (29) is inherently less than zero, we can get $\dot{V} < 0$ if the condition (13) in Theorem 1 holds. Since $V > 0$ and $\dot{V} < 0$, we get $\lim_{t \rightarrow \infty} E(t) = 0$ from (23), thus;

we conclude that $\lim_{t \rightarrow \infty} q_F = -(L_1^{-1} L_2 \otimes I_d) q_L$ according to (17).

We note that (13) presents conditions for parameters in the control law. The existing linear matrix inequalities (LMIs) method may be used to solve (13). However, (13) is not fully the form of LMIs; Therefore, a systematic method is provided to transform it into LMIs, which is detailed in Appendix A.

Remark 3: Note that Theorem 1 actually provides the sufficient condition for achieving containment control under the stated communication delay. The sufficient condition is established by Lyapunov–Krasovskii function, which can be solved by LMIs to obtain the suitable parameters in the control law.

IV. SAFETY-CRITICAL CONTROL VIA CBFs

In the previous section, we provided a control law that can achieve the containment control under time-varying and nonuniform communication delay, which is the first main concern mentioned in the Introduction. However, obstacle avoidance, which is another major concern in containment control since the position of agents is jointly determined by their neighbors and it is hard to plan safe paths in advance, has not yet been addressed. Thus, solving these two concerns simultaneously and minimize the impact of obstacle avoidance on tracking performance is the next focus of work. In this section, we achieve this goal by using CBFs-based safety-critical control method. It can be seen as a safety filter that optimizes the nominal control law proposed in Section III, thus achieving a better trade-off between safety and control performance.

A. Control Barrier Function Design

We rewrite (1) in the following form to facilitate the safety-critical control law design.

$$\dot{x}_i = f_i(x_i) + g_i(x_i)\tau_i \quad (34)$$

where $x_i = \text{col}(q_i, \dot{q}_i)$, $f_i(x_i) = \text{col}(\dot{q}_i, -M_i^{-1}(C_i\dot{q}_i + G_i))$, and $g_i(x_i) = [\mathbf{0}_{d \times d}, (M_i^{-1})^T]$.

Consider the safety set $\text{Int}(\mathcal{C}_i)$ for the i -th agent.

$$\text{Int}(\mathcal{C}_i) = \{x_i \in \mathbb{R}^{2d} : s(x_i, t) > 0\},$$

$$\partial\mathcal{C}_i = \{x_i \in \mathbb{R}^{2d} : s(x_i, t) = 0\}, \quad (35)$$

where $\partial\mathcal{C}_i$ denotes the boundary of $\text{Int}(\mathcal{C}_i)$ and $s(x_i, t)$ is a continuously differentiable function. In the context of obstacle avoidance, we can define $s(x_i, t)$ as

$$s(x_i, t) = \|q_i - q_k(t)\|_2^2 - r_k^2, \quad (36)$$

where $q_k(t) \in \mathbb{R}^d$ is the position of the k -th obstacle and r_k is the radius of the corresponding danger area.

Remark 4: r_k is the radius of the danger area corresponding to the k -th obstacle, which means that both the dimensions of the agent and the obstacles are considered; i.e., $s(x_i, t) > 0$ indicates that no collision occurred. In addition, $q_k(t)$ is a function of t , which means that the obstacles can be stationary or moving.

Definition 2 [61]: Consider the safety set $\text{Int}(\mathcal{C}_i)$ defined by $s(x_i, t)$ as described in (35); then, a continuously differentiable

function $B(x_i, t) : \text{Int}(\mathcal{C}_i) \times [t_0, \infty) \rightarrow \mathbb{R}$ is a CBF if the following conditions hold for all $x_i \in \text{Int}(\mathcal{C}_i)$ and $t \geq t_0$.

$$\frac{1}{\wp_1(s(x_i, t))} \leq B(x_i, t) \leq \frac{1}{\wp_2(s(x_i, t))}, \quad (37)$$

$$\dot{B}(x_i, t) \leq \frac{\iota}{B(x_i, t)}, \quad (38)$$

where \wp_1 and \wp_2 are class \mathcal{K} functions with respect to $s(x_i, t)$ and $\iota > 0$.

We propose a control barrier function candidate as follows:

$$B(x_i, t) = -\ln\left(\frac{s(x_i, t)}{1 + s(x_i, t)}\right) + \xi \arctan(\delta \dot{s}^2(x_i, t)), \quad (39)$$

where $\xi > 0$ and $\delta > 0$. Then, the safety-critical control set can be given as

$$\mathcal{S}_\tau = \left\{ \tau_i : \mathcal{L}_f B(x_i, t) + \mathcal{L}_g B(x_i, t) \tau_i + \frac{\partial B(x_i, t)}{\partial t} \leq \frac{\iota}{B(x_i, t)} \right\} \quad (40)$$

where $\mathcal{L}_f B(x_i, t)$ is the Lie derivative of $B(x_i, t)$ with respect to $f_i(x_i)$, which can be defined by $\mathcal{L}_f B(x_i, t) = (\partial B / \partial x_i) f_i(x_i)$. Similarly, $\mathcal{L}_g B(x_i, t) = (\partial B / \partial x_i) g_i(x_i)$.

Assumption 3: The safety set $\text{Int}(\mathcal{C}_i)$ is not empty with no isolated points, and the safety-critical control input set \mathcal{S}_τ is not empty.

Remark 5: We note that tight control input restriction may result in infeasibility, i.e., the needed input is too large and conflicts with tight input restriction. The feasibility analysis for safety-critical control is a specialized topic that requires separate efforts, as in [62] and [63]. It is worth noting that this work mainly focuses on improving the robustness of CBFs and feasibility analysis is not the focus. So the same as in [64], [65], we give the Assumption 3 and assume that the control input can be sufficiently large when activating safe behaviors.

Theorem 2: The function in (39) is a control barrier function. Furthermore, the safety-critical control set proposed in (40) results in the safety set $\text{Int}(\mathcal{C}_i)$ being forward invariant.

Proof: First, we show that (39) is a CBF, which starts by verifying the following important property of CBFs

$$\inf_{x_i \in \text{Int}(\mathcal{C}_i)} B(x_i, t) \geq 0, \lim_{x_i \rightarrow \partial\mathcal{C}_i} B(x_i, t) = \infty. \quad (41)$$

Without causing confusion, we use s_i , \dot{s}_i , and B_i to denote $s(x_i, t)$, $\dot{s}(x_i, t)$, and $B(x_i, t)$, respectively. We can note that $\xi \arctan(\delta \dot{s}_i^2) \in [0, \xi\pi/2]$ since $\delta \dot{s}_i^2 \geq 0$, $-\ln(s_i/(1+s_i)) \geq 0$ when $s_i > 0$, and $-\ln(s_i/(1+s_i)) \rightarrow \infty$ if and only if $s_i \rightarrow 0$. Therefore, we conclude that (41) holds since $s_i > 0$ means $x_i \in \text{Int}(\mathcal{C}_i)$ and $s_i \rightarrow 0$ stands for $x_i \rightarrow \partial\mathcal{C}_i$ according to (35).

Meanwhile, based on the above analysis, we have

$$\frac{1}{-\ln(s_i/(1+s_i))} \geq \frac{1}{B_i} \geq \frac{1}{-\ln(s_i/(1+s_i)) + \xi\pi/2}, \quad (42)$$

Taking the reciprocal of (42) yields

$$\frac{1}{\wp_1(s_i)} \leq B_i \leq \frac{1}{\wp_2(s_i)}, \quad (43)$$

where $\varphi_1(s_i) = 1/[-\ln(s_i/(1+s_i))]$ and $\varphi_2(s_i) = 1/[-\ln(s_i/(1+s_i)) + \xi\pi/2]$ are class \mathcal{K} functions with respect to s_i . Therefore, we can conclude that (37) holds.

Then, we focus on the condition (38), taking the derivative of (39) with respect to time, we have

$$\dot{B}_i = \mathcal{L}_f B_i + \mathcal{L}_g B_i \tau_i + \frac{\partial B_i}{\partial t}. \quad (44)$$

We note that the control input is inactive when $\mathcal{L}_g B_i = 0$, so we first consider this case. $\mathcal{L}_g B_i$ can be expanded as

$$\mathcal{L}_g B(x_i, t) = \left(\frac{\partial B_i}{\partial s_i} \frac{\partial s_i}{\partial x_i} + \frac{\partial B_i}{\partial \dot{s}_i} \frac{\partial \dot{s}_i}{\partial x_i} \right) g_i(x_i) = \frac{\partial B_i}{\partial \dot{s}_i} \frac{\partial \dot{s}_i}{\partial x_i} g_i(x_i) \quad (45)$$

where the last equation comes from $(\partial s_i / \partial x_i) g_i(x_i) = 0$.

Meanwhile, $(\partial \dot{s}_i / \partial x_i) g_i(x_i) \neq 0$; thus, $\mathcal{L}_g B_i = 0$ implies that $\partial B_i / \partial \dot{s}_i = 0$. Further calculation shows that

$$\frac{\partial B_i}{\partial \dot{s}_i} = \xi \frac{2\delta \dot{s}_i}{1 + \delta^2 \dot{s}_i^4} = 0 \rightarrow \dot{s}_i = 0. \quad (46)$$

Based on this, (44) can be further computed as

$$\begin{aligned} \dot{B}_i &= \left(\frac{\partial B_i}{\partial s_i} \frac{\partial s_i}{\partial x} + \frac{\partial B_i}{\partial \dot{s}_i} \frac{\partial \dot{s}_i}{\partial x} \right) \dot{x}_i + \frac{\partial B_i}{\partial s_i} \frac{\partial s_i}{\partial t} + \frac{\partial B_i}{\partial \dot{s}_i} \frac{\partial \dot{s}_i}{\partial t} \\ &= \frac{\partial B_i}{\partial s_i} \frac{\partial s_i}{\partial x} \dot{x}_i + \frac{\partial B_i}{\partial s_i} \frac{\partial s_i}{\partial t} = \frac{\partial B_i}{\partial s_i} \dot{s}_i = 0 \end{aligned} \quad (47)$$

where the second equation comes from $\dot{s}_i = 0$. Therefore, we conclude that (38) holds in this case since $\iota > 0$ and $B_i \geq 0$.

Then, we consider the case $\mathcal{L}_g B(x_i, t) \neq 0$, which means that the control input can be used to change the value of B_i . From Assumption 3, we know that there always exists a control input such that B_i satisfies the conditions described in (38). Based on the above discussion, we know that (38) holds. Thus, the B_i presented in (39) is a control barrier function.

Second, we show that control inputs in the safety-critical control set \mathcal{S}_τ lead to the safety set $\text{Int}(\mathcal{C}_i)$ being forward invariant. (42) shows $B_i \geq -\ln(s_i/(1+s_i)) \geq 0$. Then, the control inputs in \mathcal{S}_τ lead to

$$\dot{B}_i \leq \frac{\iota}{B_i} \leq \frac{\iota}{-\ln(s_i/(1+s_i))}, \quad (48)$$

where $\iota/[-\ln(s_i/(1+s_i))]$ is a class \mathcal{K} function, and we denote it as $\varphi_3(s_i)$.

Combining (37), (38), and (48), we have

$$\dot{B}_i \leq \varphi_3 \circ \varphi_2^{-1}(1/B_i), \quad (49)$$

where $\varphi_3 \circ \varphi_2^{-1}$ is a class \mathcal{K} function. According to the analysis in [66], we obtain

$$B_i \leq \frac{1}{\lambda(1/B_i(x_{i,0}, t_0), t - t_0)} \quad (50)$$

for all $t \geq t_0$, where λ is a class \mathcal{KL} function and $x_{i,0}$ stands for $x_i(t_0)$. Based on (37), (50), and the properties of the class \mathcal{K} function and class \mathcal{KL} function, we get

$$s \geq \varphi_1^{-1} \circ \lambda(1/B(x_{i,0}, t_0), t - t_0) \geq 0 \quad (51)$$

for $t \geq t_0$ if $x_{i,0} \in \text{Int}(\mathcal{C}_i)$. In other words, $x_i \in \text{Int}(\mathcal{C}_i)$ for all $t \geq t_0$ if $x_{i,0} \in \text{Int}(\mathcal{C}_i)$, which means that $\text{Int}(\mathcal{C}_i)$ is forward invariant with the control input in \mathcal{S}_τ . ■

Remark 6: We note that (39) is a well-designed CBF for EL system with position-based safety constraints, i.e., a system with relative degree 2. Compared with existing work [67], [68], it simplifies the design process for the above systems and, more importantly, facilitates achieving state constraints.

B. Robust Safety-Critical Control Law Design

Theorem 2 shows that satisfying the safety condition in (40) leads to the safety set being forward invariant, which means that obstacle avoidance is achieved. However, the model uncertainty in $f_i(x_i)$ make (40) ambiguous and render it difficult to determine the control input. To address this problem, we propose an observer-based robust CBF that can construct safety constraints despite uncertainties.

First, we rewrite the derivative of $B(x_i, t)$ as

$$\dot{B}_i = \mathcal{L}_{\bar{f}} B_i + \mathcal{L}_g B_i \tau_i + \Delta_i + \frac{\partial B_i}{\partial t} \quad (52)$$

where Δ_i denotes the uncertainty term in \dot{B}_i caused by the uncertainty of $f_i(x_i)$, which is defined as $\Delta_i = \mathcal{L}_f B_i - \mathcal{L}_{\bar{f}} B_i$, with $\bar{f}_i(x_i)$ being the nominal value of $f_i(x_i)$.

Then, we propose an observer to estimate the value of Δ_i

$$\begin{aligned} \hat{\Delta}_i &= k_1 B_i - \eta \\ \dot{\eta} &= k_1 \left(\mathcal{L}_{\bar{f}} B_i + \mathcal{L}_g B_i \tau_i + \hat{\Delta}_i + \frac{\partial B_i}{\partial t} \right) \end{aligned} \quad (53)$$

where $k_1 > 0$ is the observer gain.

Lemma 3: Given the uncertainty term Δ_i in (52), using the observer (53), the estimate error $\varepsilon_i = \Delta_i - \hat{\Delta}_i$ is convergent and can be quantified as

$$|\varepsilon_i| \leq \left(|\varepsilon_{i,0}| - \frac{l_i}{k_1} \right) e^{-k_1 t} + \frac{l_i}{k_1} \quad (54)$$

where $\varepsilon_{i,0} = \varepsilon_i(0)$ and l_i is the Lipschitz constant of Δ_i . ■

Proof: See Appendix B.

Since the estimation error is convergent, we can use $\hat{\Delta}_i$ to replace the unknown Δ_i in (52). Nevertheless, the effect of estimation error needs to be considered to enforce robustness. According to Lemma 3, we conclude that (53) is an observer with quantified estimation error, which means that there exists a function $N_i(t)$ satisfying $|\varepsilon_i| \leq N_i(t)$. Based on (54), $N_i(t)$ can be chosen as $N_i(t) = \sigma_i e^{-k_1 t} + l_i/k_1$ with $\sigma_i \geq |\varepsilon_{i,0}| - l_i/k_1$.

Then, we incorporate the estimate into the safety constraint in (40), and the robust safety condition can be rewritten as

$$\mathcal{L}_{\bar{f}} B_i + \mathcal{L}_g B_i \tau_i + \hat{\Delta}_i + N_i(t) + \frac{\partial B_i}{\partial t} \leq \frac{\iota}{B_i}, \quad (55)$$

where $N_i(t)$ is actually a robust term, which is introduced to cancel out the estimation error. Therefore, we conclude that the τ_i satisfying (55) leads to $\tau_i \in \mathcal{S}_\tau$ despite uncertainty.

Remark 7: As mentioned above, CBFs commonly depend on accurate models, and their application to uncertain systems is a problem being studied. Compared to existing data-driven [47],

[69] and worst case-based [45], [70] methods, observer-based robust CBF can avoid overly conservative behavior at a lower computational cost. The less conservative and more fully guaranteed performance of this observer-based CBF is obvious since it provides robustness with the estimate of the uncertainty rather than the bound of the uncertainty in [45], [70]. Regarding the computational efficiency compared to GP-based CBF, we can verify our conclusion with computational complexity theory. We can see that the GP prediction used in [47], [69] is a data-driven method and its basic complexity is $\mathcal{O}(n^3)$ due to the inverse computation of a $n \times n$ matrix. We refer interested readers to [51] for more details. In comparison, the observer used in this paper is an estimation method, and the main computational complexity of (53) comes from the numerical integration, which can be solved by the Clenshaw–Curtis quadrature with the complexity of only $\mathcal{O}(n \log n)$. We refer interested readers to [71], [72] for more details. Thus, the complexity analysis shows that observer-based CBF has less computational burden than the GP-based CBF, and we also execute comparative experiment in Section V to intuitively show this point.

With the robust safety condition (55), safety-critical control can be transformed into an optimal control problem subject to multiple safety constraints corresponding to numerous obstacles. Specifically, the nominal containment control law $\bar{\tau}_i$ in (11) can be optimized via a quadratic program (QP).

$$\begin{aligned} \tau_i &= \arg \min \| \tau_i - \bar{\tau}_i \|^2 \\ \text{s.t. } A_i(x_i) \tau_i &\leq b_i(x_i) \end{aligned} \quad (56)$$

where $A_i(x_i) = \mathcal{L}_g B_i$, and $b_i(x_i) = \iota/B_i - \partial B_i/\partial t - \mathcal{L}_f B_i - \hat{\Delta}_i - N_i(t)$.

Remark 8: Note that obstacle avoidance is achieved via optimal control, which can better synthesize multiple conflicts between safety constraints and control performance. Therefore, containment tracking performance is minimally affected while achieving obstacle avoidance behavior.

V. SIMULATION RESULTS

Consider an MAS with 4 leaders and 10 followers moving in the 2-D plane, whose dynamic is described by (1). The $M_i(q_i)$, $C_i(q_i, \dot{q}_i)$, and $G_i(q_i)$ are the same as in [73] with $[M]_{(1,1)} = a_1 + 2a_2 \cos q(2)$, $[M]_{(1,2)} = [M]_{(2,1)} = a_3 + a_2 \cos q(1)$, $[M]_{(2,2)} = a_3$, $[C]_{(1,1)} = -2a_2 \sin q(2)\dot{q}(2)$, $[C]_{(1,2)} = [C]_{(2,1)} = -a_2 + \sin q(1)\dot{q}(1)$, $[C]_{(2,2)} = 0$, and $G = [0, 0]^T$. The unknown true model parameters are $a_1 = 1.3$, $a_2 = 0.06$, and $a_3 = 0.3$, and the nominal model parameters that are known and can be used in the control law design are specified as $a_1 = 1 + \delta_m$, $a_2 = 0.1 + \delta_m$, and $a_3 = 0.5 + \delta_m$, where δ_m is noise random series in $(-0.1, 0.1)$.

The communication topology of agents is illustrated in Fig. 1, and the communication delays are characterized as $T_{11,1}(t) = T_{12,2}(t) = 0.2 \cos(t) + 0.1 + \delta$, $T_{11,4}(t) = T_{14,3}(t) = 0.1 \cos(t) + 0.2 + \delta$, $T_{12,1}(t) = T_{13,2}(t) = T_{1,5}(t) = T_{1,7}(t) = 0.2 \cos(t) + 0.2 + \delta$, $T_{1,2}(t) = T_{3,4}(t) = T_{4,1}(t) = T_{2,3}(t) = 0.1 \sin(t) + 0.2 + \delta$, $T_{4,5}(t) = T_{4,8}(t) = T_{2,6}(t) = T_{3,6}(t) = 0.2 \sin(t) + 0.1 \cos(0.5t) + 0.1 + \delta$, $T_{13,3}(t) = T_{14,4}(t) = T_{2,7}$

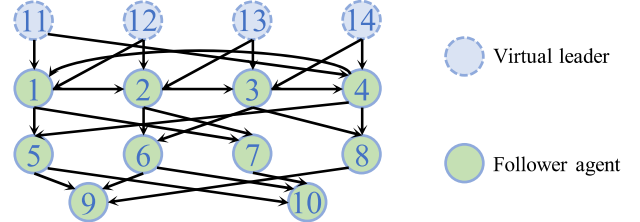


Fig. 1. Communication topology.

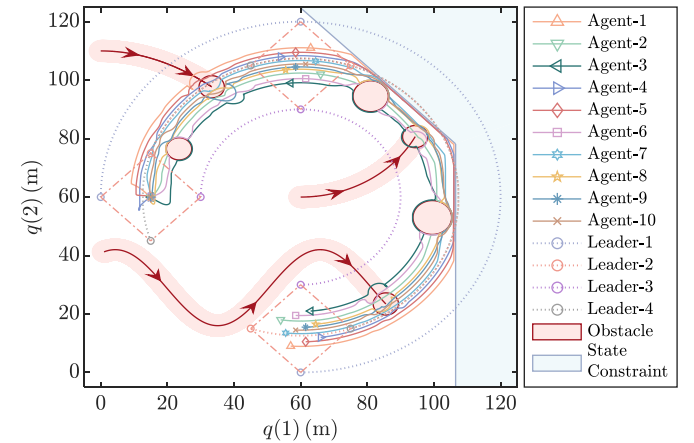


Fig. 2. The moving paths of agents.

$(t) = T_{3,8}(t) = 0.1 \sin(0.6t) + 0.15 \cos(0.7t) + \delta$, $T_{5,9}(t) = T_{6,9}(t) = T_{8,9}(t) = 0.1 \sin(0.95t) + 0.16 + \delta$, and $T_{5,10}(t) = T_{6,10}(t) = T_{7,10}(t) = 0.25 \sin(0.4t) + 0.1 \cos(0.6t) + \delta$, where δ is noise generated by random series in $(0, 0.1)$. Four leaders span a quadrilateral whose center moves along a circle with a radius of 45 and a center at $(60, 60)$. From the above delays, by using the LMI solver in MATLAB, we get the parameters in control law as $\sigma = 0.52$ and $\lambda = 0.86$. The initial conditions for follower agents are $q_i = [15, 60]^T$, $\dot{q}_i = [0, 0]^T$, $i = 1, \dots, 8$.

Multiple stationary and moving obstacles are placed in the moving path to create collision threats, whose positions are described as $q_{ob1} = [23.5, 76.5]^T$, $q_{ob2} = [0.18t, -3.6 \times 10^{-4} \times t^2]^T$, $q_{ob3} = [81, 94.5]^T$, $q_{ob4} = [60 + 39 \sin 0.002t, 99 - 39 \cos 0.002t]^T$, $q_{ob5} = [99.5, 53.2]^T$, and $q_{ob6} = [0.1t, 13 \sin(0.01t - 5) + 30]^T$, and the radius of the danger area are $r_i = 4$, $i = 1, 2, 4, 6$, $r_3 = 5.5$, and $r_5 = 6$. Meanwhile, two state constraints are set as $q(1) + q(2) \leq 184$ and $q(1) \leq 106$. Then, eight CBFs are formulated corresponding to six safety concerns and two state constraints. Specifically, $s_k = \|q - q_{obk}\|_2^2 - r_k^2$, $k = 1, \dots, 6$, $s_7 = -q(1) + 106$, and $s_8 = -q(1) - q(2) + 184$. The parameters in robust CBF are designed as $\xi = 0.1$, $\delta = 0.1$, $\iota = 30$, and $k_1 = 5$.

All experiments are executed on a laptop with Intel Core i9-13900, RAM 16GB, and GPU 4060. The simulation running time is 900 s, and the simulation results are shown in Figs. 2–6. Fig. 2 shows the moving paths of agents with time-varying velocities, we see that all followers can enter the convex hull spanned by virtual leaders despite nonuniform time-varying

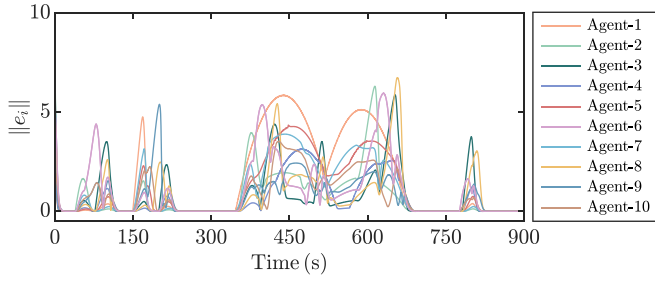


Fig. 3. The containment tracking error.

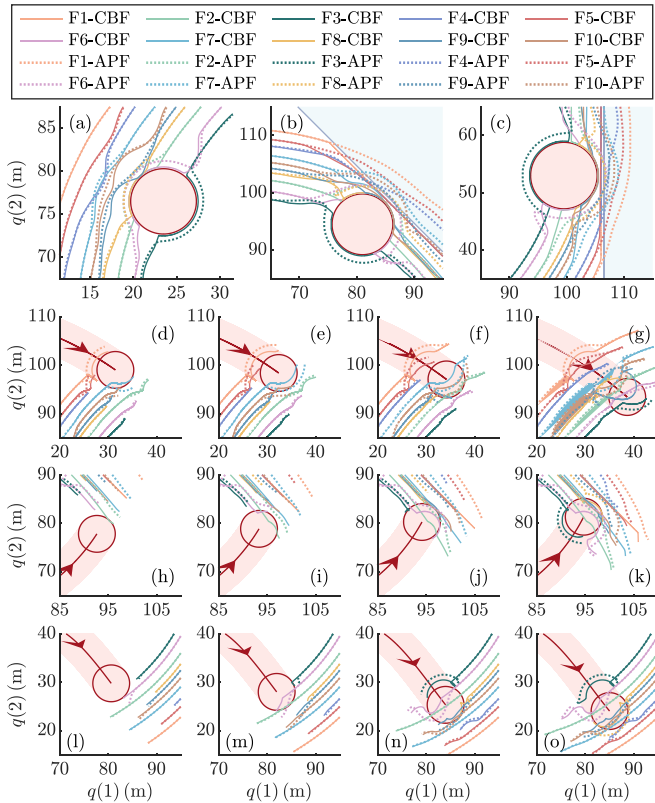


Fig. 4. Snapshots during obstacle avoidance process. (a) $t = 10 \sim 106$ s, (b) $t = 297 \sim 439$ s, (c) $t = 551 \sim 691$ s, (d) $t = 170$ s, (e) $t = 180$ s, (f) $t = 190$ s, (g) $t = 215$ s, (h) $t = 475$ s, (i) $t = 490$ s, (j) $t = 510$ s, (k) $t = 525$ s, (l) $t = 777$ s, (m) $t = 790$ s, (n) $t = 810$ s, (o) $t = 820$ s.

communication delays; moreover, all followers can avoid multiple static and moving obstacles, and the state constraints remain unviolated. Fig. 3 shows the containment tracking errors, we see that the tracking errors of all agents converge to 0 when there are no safety threats and state constraints. To demonstrate the superiority of the CBF-based method for obstacle avoidance, we compare our method with the method using APF in [36], and several snapshots during obstacle avoidance are shown in Fig. 4. We can see that both APF and CBF-based methods can achieve obstacle avoidance. However, compared to the APF, we note that the CBF only works when a collision is imminent; therefore, the tracking performance is much less affected. Moreover, we note that APF-based methods violate the state constraints; in contrast, the CBF-based methods benefit from optimal control

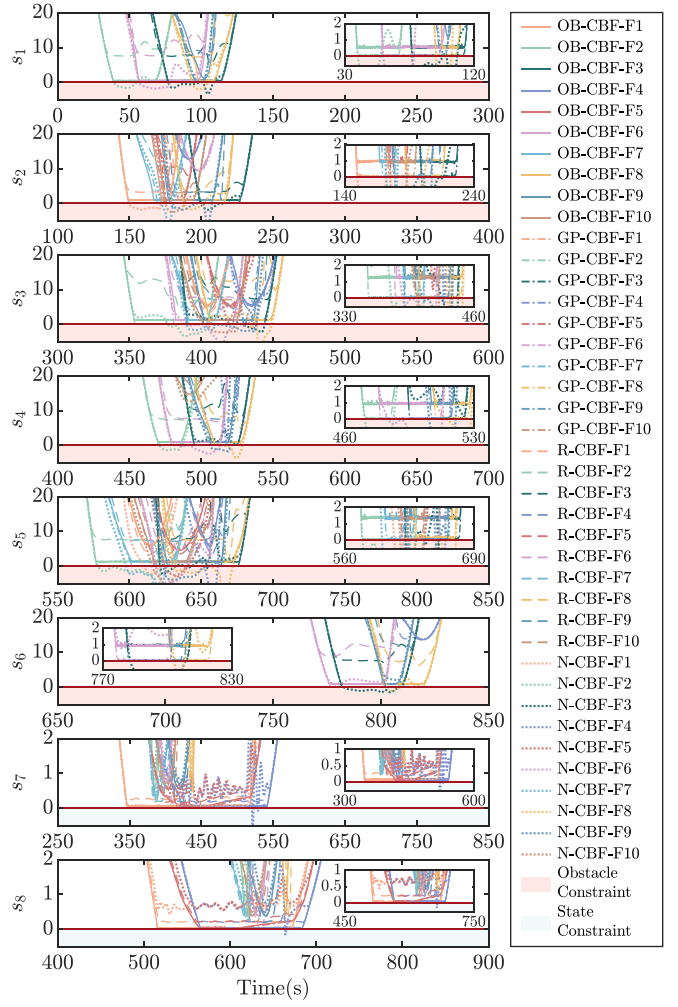


Fig. 5. The values of function s_i .

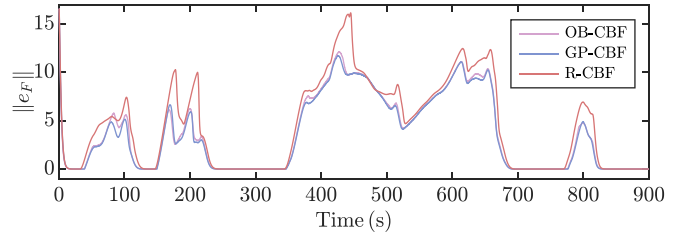


Fig. 6. The tracking errors using OB-CBF, R-CBF, and GP-CBF.

and can better synthesize the conflicts between safety, state constraints, and control performance. We need to clarify that in subfigure (d)-(o), since the obstacle is moving, the path crossing obstacles does not mean that the collision has occurred, and the collision-free behavior can be verified later in Fig. 5.

Furthermore, we compare our method, the observer-based CBF (OB-CBF), with the other three CBFs. To make explicit, the other three CBFs are the robust CBF (R-CBF) proposed in [45], which considers the worst case and uses the bound of uncertainty to build safety conditions; the Gaussian Process-based CBF (GP-CBF) proposed in [47], which uses the GP to predict the uncertainty emerging in the CBF; and

the nominal dynamics-based CBF (N-CBF), which constructs the safety conditions using the nominal dynamic and has no additional measures to deal with model uncertainty. Fig. 5 shows the values of function s_i , we can see that the N-CBF violates the safety and state constraints since it is constructed by using the nominal dynamics; thus the uncertainty between the nominal and true dynamics has a negative impact on safety constraints and leads to system unsafety. As a comparison, the OB-CBF in this paper, which is constructed using the nominal dynamics and the uncertainty estimation, can ensure system safety and satisfy state constraints. Moreover, we note that the R-CBF and the GP-CBF can also provide system security. However, compared to the OB-CBF, the R-CBF is overly conservative than needed, which reduces the choice of control actions and thus affects the control performance. The GP-CBF achieves slightly better behavior than the OB-CBF, but at the cost of a high computational cost, with 85ms needed to solve one single step when using the GP-CBF, compared to 9ms when using the OB-CBF. Fig. 6 shows the tracking errors using OB-CBF, R-CBF, and GP-CBF, we can see that the OB-CBF provides a better tradeoff between safety and control performance at a lower computational cost.

VI. CONCLUSION

In this paper, we addressed the containment control problem for MASs subject to nonuniform time-varying communication delay. We removed the existing restrictions that the delay can only be uniform in dynamic formation configuration and agents are modeled by linear systems under these complex delay conditions. Moreover, we proposed a robust CBF-based safety-critical control method for obstacle avoidance, which takes advantage of optimization control to achieve a better balance of safety and performance. In addition, facing adverse effects of uncertainty on safety constraints, we proposed an observer with quantified error to provide CBF with robustness against uncertainty. Several sets of comparative experiments illustrated the advantages of this work over existing results.

APPENDIX A

We note that $\bar{\Theta} < 0$ and $\bar{\Pi} < 0$ are not LMIs and cannot be calculated by using existing numerical methods. Nevertheless, we provide a systematic approach to transform them into LMIs. We present $\bar{\Theta} < 0$ as an example, and $\bar{\Pi} < 0$ can be calculated in the same way.

First, by pre- and post-multiplying the matrix $\bar{\Theta}$ by matrix $\text{diag}\{\hat{P}_1^{-1}, \hat{P}_2^{-1}, I, \hat{P}_3^{-1}\}$ and by letting $Q_1 = P_1$ and $Q_2 = P_2$, we obtain a symmetric matrix Γ with

$$\Gamma_{(1,1)} = \hat{P}_1^{-1} \hat{A}^T + \hat{A} \hat{P}_1^{-1} + \hat{P}_1^{-1} \hat{P}_2 \hat{P}_1^{-1} + 2 \hat{P}_1^{-1},$$

$$\Gamma_{(1,2)} = X \hat{B}_a \hat{P}_2^{-1} + \hat{P}_1^{-1} - \hat{P}_2^{-1}$$

$$\Gamma_{(1,3)} = \hat{P}_1^{-1} \hat{A}^T, \Gamma_{(1,4)} = \hat{P}_3^{-1}, \Gamma_{(2,2)} = (\gamma - 3) \hat{P}_2^{-1},$$

$$\Gamma_{(2,3)} = X \hat{P}_2^{-1} \hat{B}_a^T,$$

$$\Gamma_{(2,4)} = \hat{P}_3^{-1}, \Gamma_{(3,3)} = -\varphi^{-1} \hat{P}_3^{-1}, \Gamma_{(3,4)} = 0,$$

$$\Gamma_{(4,4)} = -\varphi^{-1} \hat{P}_3^{-1},$$

and we see that $\bar{\Theta} < 0$ is equivalent to $\Gamma < 0$.

Then, we use variable substitution, letting $\hat{Z}_i = \hat{P}_i^{-1}, i = 1, 2, 3$ and $W = \hat{B}_a \hat{Z}_2$. Meanwhile, according to Schur's Lemma, we have $\Gamma < 0$ is equivalent to $\bar{\Gamma} < 0$, where $\bar{\Gamma}$ is a symmetric matrix defined as

$$\bar{\Gamma}_{(1,1)} = \hat{Z}_1 \hat{A}^T + \hat{A} \hat{Z}_1 + 2 \hat{Z}_1, \bar{\Gamma}_{(1,2)}$$

$$= X W + \hat{Z}_1 - \hat{Z}_2, \bar{\Gamma}_{(1,3)} = \hat{Z}_1 \hat{A}^T,$$

$$\bar{\Gamma}_{(1,4)} = \hat{Z}_3, \bar{\Gamma}_{(1,5)} = \hat{Z}_1, \bar{\Gamma}_{(2,2)}$$

$$= (\gamma - 3) \hat{Z}_2, \bar{\Gamma}_{(2,3)} = X W^T,$$

$$\bar{\Gamma}_{(2,4)} = \hat{Z}_3, \bar{\Gamma}_{(3,3)} = -\varphi^{-1} \hat{Z}_3, \bar{\Gamma}_{(4,4)} = -\varphi^{-1} \hat{Z}_3, \bar{\Gamma}_{(5,5)} = -\hat{Z}_2,$$

where the other terms are zero matrices.

In this way, $\bar{\Theta} < 0$ is equivalently transformed into $\bar{\Gamma} < 0$, which is an LMI that can be solved by using existing numerical methods; thus, the control parameters in \hat{B}_a can be determined by $\hat{B}_a = W \hat{Z}_2^{-1}$.

APPENDIX B

According to (52) and (53), we have

$$\dot{\hat{\Delta}}_i = k_1(\Delta_i - \hat{\Delta}_i), \quad (57)$$

whose solution can be given by

$$\hat{\Delta}_i(t) = \hat{\Delta}_i(0) e^{-k_1 t} + \int_0^t e^{-k_1(t-r)} k_1 \Delta_i(r) dr. \quad (58)$$

In this way, we get the solution of the estimate error

$$\varepsilon_i(t) = \Delta_i(t) - \Delta_i(0) e^{-k_1 t} + \varepsilon_{i,0} e^{-k_1 t} - \int_0^t e^{-k_1(t-r)} k_1 \Delta(r) dr \quad (59)$$

where the term $\Delta_i(t) - \Delta_i(0) e^{-k_1 t}$ can be further calculated as

$$\begin{aligned} & \Delta_i(t) - \Delta_i(0) e^{-k_1 t} \\ &= \Delta_i(r) e^{-k_1(t-r)}|_0^t \\ &= \int_0^t e^{-k_1(t-r)} k_1 \Delta_i(r) dr + \int_0^t e^{-k_1(t-r)} d\Delta_i(r). \end{aligned} \quad (60)$$

Substituting (60) into (59), we get

$$\varepsilon_i(t) = \varepsilon_{i,0} e^{-k_1 t} + \int_0^t e^{-k_1(t-r)} d\Delta_i(r), \quad (61)$$

where the last term satisfies

$$\left| \int_0^t e^{-k_1(t-r)} d\Delta_i(r) \right| \leq \int_0^t l_i e^{-k_1(t-r)} dr = \frac{l_i}{k_1} (1 - e^{-k_1 t}). \quad (62)$$

By combining (61) and (62), we obtain (54).

REFERENCES

- [1] Z. Du, Z. Wu, Y. Kao, Q. Jia, and Z. Qu, "Event-triggered fuzzy controller co-design for networked systems with denial-of-service attacks and its applications," *Expert Syst. Appl.*, vol. 245, Jul. 2024, Art. no. 123072.

- [2] C. Chen, Y. Han, S. Zhu, and Z. Zeng, "Distributed fixed-time tracking and containment control for second-order multi-agent systems: A nonsingular sliding-mode control approach," *IEEE Trans. Netw. Sci. Eng.*, vol. 10, no. 2, pp. 687–697, Mar./Apr. 2023.
- [3] Z. Yu, Z. Liu, Y. Zhang, Y. Qu, and C.-Y. Su, "Distributed finite-time fault-tolerant containment control for multiple unmanned aerial vehicles," *IEEE Trans. Neural Netw. Learn. Syst.*, vol. 31, no. 6, pp. 2077–2091, Jun. 2020.
- [4] B. Cui, Y. Xia, K. Liu, J. Zhang, Y. Wang, and G. Shen, "Truly distributed finite-time attitude formation-containment control for networked uncertain rigid spacecraft," *IEEE Trans. Cybern.*, vol. 52, no. 7, pp. 5882–5896, Jul. 2022.
- [5] J. Yan, S. Peng, X. Yang, X. Luo, and X. Guan, "Containment control of autonomous underwater vehicles with stochastic environment disturbances," *IEEE Trans. Syst., Man, Cybern.: Syst.*, vol. 53, no. 9, pp. 5809–5820, Sep. 2023.
- [6] Y. Mao, Y. Gu, N. Hovakimyan, L. Sha, and P. Voulgaris, "S ℓ_1 -simplex: Safe velocity regulation of self-driving vehicles in dynamic and unforeseen environments," *ACM Trans. Cyber-Phys. Syst.*, vol. 7, no. 1, pp. 1–24, Jan. 2023.
- [7] L. Long and J. Wang, "Safety-critical dynamic event-triggered control of nonlinear systems," *Syst. Control Lett.*, vol. 162, Apr. 2022, Art. no. 105176.
- [8] A. D. Ames, X. Xu, J. W. Grizzle, and P. Tabuada, "Control barrier function based quadratic programs for safety critical systems," *IEEE Trans. Autom. Control*, vol. 62, no. 8, pp. 3861–3876, Aug. 2017.
- [9] A. D. Ames et al., "Control barrier functions: Theory and applications," in *Proc. IEEE Eur. Control Conf.*, 2019, pp. 3420–3431.
- [10] W. Li, L. Xie, and J.-F. Zhang, "Containment control of leader-following multi-agent systems with Markovian switching network topologies and measurement noises," *Automatica*, vol. 51, pp. 263–267, Jan. 2015.
- [11] H. Su and L. Zhang, "Model-independent containment control for dynamic multiple euler-lagrange systems with disturbances and uncertainties," *IEEE Trans. Netw. Sci. Eng.*, vol. 8, no. 4, pp. 3443–3452, Oct. 2021.
- [12] X. Gong, Y. Cui, J. Shen, Z. Feng, and T. Huang, "Necessary and sufficient conditions of formation-containment control of high-order multiagent systems with observer-type protocols," *IEEE Trans. Cybern.*, vol. 52, no. 7, pp. 7002–7016, Jul. 2022.
- [13] C. Lu, H. Ma, Y. Pan, Q. Zhou, and H. Li, "Observer-based finite-time fault-tolerant control for nonstrict-feedback nonlinear systems with multiple uncertainties," *IEEE Trans. Syst., Man, Cybern., Syst.*, vol. 53, no. 8, pp. 4912–4921, Aug. 2023.
- [14] Y. Liu, H. Zhang, Z. Shi, and Z. Gao, "Neural-network-based finite-time bipartite containment control for fractional-order multi-agent systems," *IEEE Trans. Neural Netw. Learn. Syst.*, vol. 34, no. 10, pp. 7418–7429, Oct. 2023.
- [15] Y. Qu, W. Zhao, Z. Yu, and B. Xiao, "Distributed prescribed performance containment control for unmanned surface vehicles based on disturbance observer," *ISA Trans.*, vol. 125, pp. 699–706, Jun. 2022.
- [16] Z. Wang, X. Wang, and C. Zhao, "Event-triggered containment control for nonlinear multiagent systems via reinforcement learning," *IEEE Trans. Circuits Syst. II, Exp. Briefs*, vol. 70, no. 8, pp. 2904–2908, Aug. 2023.
- [17] S. Xiao and J. Dong, "Distributed fault-tolerant containment control for nonlinear multi-agent systems under directed network topology via hierarchical approach," *IEEE/CAA J. Automat. Sinica*, vol. 8, no. 4, pp. 806–816, Apr. 2021.
- [18] K. Pang, L. Ma, H. Bai, and S. Xue, "Finite-time containment control for nonlinear second-order multiagent system under directed topology," *IEEE Syst. J.*, vol. 16, no. 4, pp. 6175–6184, Dec. 2022.
- [19] B. Liu, Y. Guo, and A. Li, "Nussbaum-based finite-time containment control for multi-UAVs with input saturation and velocity constraints," *Aerospace Sci. Technol.*, vol. 139, Aug. 2023, Art. no. 108407.
- [20] L. Yan, B. Ma, Y. Jia, and Y. Fu, "Adaptive containment control of multiple underactuated hovercrafts subjected to switching and directed topologies," *IEEE Syst. J.*, vol. 17, no. 3, pp. 3962–3973, Sep. 2023.
- [21] H. Liang, L. Zhang, Y. Sun, and T. Huang, "Containment control of semi-markovian multiagent systems with switching topologies," *IEEE Trans. Syst., Man, Cybern., Syst.*, vol. 51, no. 6, pp. 3889–3899, Jun. 2021.
- [22] A. Stephen, R. Karthikeyan, C. Sowmiya, R. Raja, and R. P. Agarwal, "Sampled-data controller scheme for multi-agent systems and its application to circuit network," *Neural Netw.*, vol. 170, pp. 506–520, Feb. 2024.
- [23] A. Stephen, R. Raja, X. Bai, J. Alzabut, R. Swaminathan, and G. Rajchakit, "Asymptotic pinning synchronization of nonlinear multi-agent systems: Its application to tunnel diode circuit," *Nonlinear Anal.-Hybrid Syst.*, vol. 49, Aug. 2023, Art. no. 101366.
- [24] Y. Yang and W. Hu, "Containment control of double-integrator multi-agent systems with time-varying delays," *IEEE Trans. Netw. Sci. Eng.*, vol. 9, no. 2, pp. 457–466, Mar. 2022.
- [25] Y. Cao, Y. Kao, J. H. Park, and H. Bao, "Global mittag-leffler stability of the delayed fractional-coupled reaction-diffusion system on networks without strong connectedness," *IEEE Trans. Neural Netw. Learn. Syst.*, vol. 33, no. 11, pp. 6473–6483, Nov. 2022.
- [26] Z. Ma, J. Qi, M. Wang, C. Wu, J. Guo, and S. Yuan, "Time-varying formation tracking control for multi-UAV systems with directed graph and communication delays," in *Proc. Chin. Control Conf.*, 2021, pp. 5436–5441.
- [27] D. Wang, Y. Huang, S. Guo, and W. Wang, "Distributed H_∞ containment control of multiagent systems over switching topologies with communication time delay," *Int. J. Robust Nonlinear Control*, vol. 30, no. 13, pp. 5221–5232, Sep. 2020.
- [28] M. Parsa and M. Danesh, "Robust containment control of uncertain multi-agent systems with time-delay and heterogeneous lipschitz nonlinearity," *IEEE Trans. Syst., Man, Cybern., Syst.*, vol. 51, no. 4, pp. 2312–2321, Apr. 2021.
- [29] L. Chen, C. Li, Y. Guo, G. Ma, Y. Li, and B. Xiao, "Formation-containment control of multi-agent systems with communication delays," *ISA Trans.*, vol. 128, pp. 32–43, Sep. 2022.
- [30] L. Feng, B. Huang, J. Sun, X. Xie, H. Zhang, and J. Ren, "Multi-stage dynamic event-triggered containment control of nonlinear multi-agent systems with input-bounded leaders and time-varying delay," *Int. J. Robust Nonlinear Control*, vol. 33, no. 1, pp. 574–591, Jan. 2023.
- [31] W. Li, M. Shi, L. Shi, B. Lin, and K. Qin, "Containment tracking for networked agents subject to nonuniform communication delays," *IEEE Trans. Netw. Sci. Eng.*, vol. 10, no. 6, pp. 3658–3669, Nov. 2023.
- [32] H. Wang, H. Li, Y. Feng, and Y. Li, "Fixed-time coordinated guidance for containment maneuvering of unmanned surface vehicles under delayed communications: Theory and experiment," *Ocean Eng.*, vol. 277, Jun. 2023, Art. no. 114249.
- [33] G. De Tommasi, D. G. Lui, A. Petrillo, and S. Santini, "A L2-gain robust PID-like protocol for time-varying output formation-containment of multi-agent systems with external disturbance and communication delays," *IET Control Theory Appl.*, vol. 15, no. 9, pp. 1169–1184, Jun. 2021.
- [34] A. Yang, X. Liang, Y. Hou, and M. Lv, "An autonomous cooperative interception method with angle constraints using a swarm of UAVs," *IEEE Trans. Veh. Technol.*, vol. 72, no. 12, pp. 15436–15449, Dec. 2023.
- [35] N. Gu, D. Wang, Z. Peng, and L. Liu, "Observer-based finite-time control for distributed path maneuvering of underactuated unmanned surface vehicles with collision avoidance and connectivity preservation," *IEEE Trans. Syst., Man, Cybern., Syst.*, vol. 51, no. 8, pp. 5105–5115, Aug. 2021.
- [36] L. Chen and H. Duan, "Collision-free formation-containment control for a group of UAVs with unknown disturbances," *Aerospace Sci. Technol.*, vol. 126, Jul. 2022, Art. no. 107618.
- [37] L. Wang, A. D. Ames, and M. Egerstedt, "Safety barrier certificates for collisions-free multirobot systems," *IEEE Trans. Robot.*, vol. 33, no. 3, pp. 661–674, Jun. 2017.
- [38] S. Kousik, S. Vaskov, F. Bu, M. Johnson-Roberson, and R. Vasudevan, "Bridging the gap between safety and real-time performance in receding-horizon trajectory design for mobile robots," *Int. J. Rob. Res.*, vol. 39, no. 12, pp. 1419–1469, Oct. 2020.
- [39] P. Akella, W. Ubellacker, and A. D. Ames, "Safety-critical controller verification via Sim2Real gap quantification," in *Proc. IEEE Int. Conf. Robot. Autom.*, 2023, pp. 10539–10545.
- [40] B. Li, S. Wen, Z. Yan, G. Wen, and T. Huang, "A survey on the control lyapunov function and control barrier function for nonlinear-affine control systems," *IEEE/CAA J. Automat. Sinica*, vol. 10, no. 3, pp. 584–602, Mar. 2023.
- [41] F. Califano, "Passivity-preserving safety-critical control using control barrier functions," *IEEE Control Syst. Lett.*, vol. 7, pp. 1742–1747, 2023.
- [42] A. Singletary, S. Kolathaya, and A. D. Ames, "Safety-critical kinematic control of robotic systems," *IEEE Control Syst. Lett.*, vol. 6, pp. 139–144, 2022.
- [43] G. Lv, Z. Peng, L. Liu, and J. Wang, "Barrier-certified distributed model predictive control of under-actuated autonomous surface vehicles via neuromodynamic optimization," *IEEE Trans. Syst., Man, Cybern., Syst.*, vol. 53, no. 1, pp. 563–575, Jan. 2023.
- [44] T. Jin, X. Wang, H. Ji, J. Di, and H. Yan, "Collision avoidance for multiple quadrotors using elastic safety clearance based model predictive control," in *Proc. IEEE Int. Conf. Robot. Autom.*, 2022, pp. 265–271.
- [45] Q. Nguyen and K. Sreenath, "Robust safety-critical control for dynamic robotics," *IEEE Trans. Autom. Control*, vol. 67, no. 3, pp. 1073–1088, Mar. 2022.

- [46] S. Kolathaya and A. D. Ames, "Input-to-State safety with control barrier functions," *IEEE Control Syst. Lett.*, vol. 3, no. 1, pp. 108–113, Jan. 2019.
- [47] P. Jagtap, G. J. Pappas, and M. Zamani, "Control barrier functions for unknown nonlinear systems using Gaussian processes," in *Proc. IEEE Conf. Decis. Control*, 2020, pp. 3699–3704.
- [48] Z. Wu, R. Yang, L. Zheng, and H. Cheng, "Safe learning-based feedback linearization tracking control for nonlinear system with event-triggered model update," *IEEE Rob. Autom. Lett.*, vol. 7, no. 2, pp. 3286–3293, Apr. 2022.
- [49] Y. Kao, Y. Cao, and Y. Chen, "Projective synchronization for uncertain fractional reaction-diffusion systems via adaptive sliding mode control based on finite-time scheme," *IEEE Trans. Neural Netw. Learn. Syst.*, early access, Aug. 10, 2023, doi: [10.1109/TNNLS.2023.3288849](https://doi.org/10.1109/TNNLS.2023.3288849).
- [50] P. Zhao, Y. Mao, C. Tao, N. Hovakimyan, and X. Wang, and Ieee, "Adaptive robust quadratic programs using control Lyapunov and barrier functions," in *Proc. IEEE Conf. Decis. Control*, 2020, pp. 3353–3358.
- [51] C. E. Rasmussen and C. K. I. Williams, *Gaussian Processes for Machine Learning*. Cambridge, MA, USA: MIT Press, 2006.
- [52] Q. Han, Z. Liu, H. Su, and X. Liu, "Filter-based disturbance observer and adaptive control for Euler-Lagrange systems with application to a quadrotor UAV," *IEEE Trans. Ind. Electron.*, vol. 70, no. 8, pp. 8437–8445, Aug. 2023.
- [53] S. Roy, S. B. Roy, and I. N. Kar, "Adaptive-robust control of Euler-Lagrange systems with linearly parametrizable uncertainty bound," *IEEE Trans. Control Syst. Technol.*, vol. 26, no. 5, pp. 1842–1850, Sep. 2018.
- [54] C. Zhu, B. Huang, B. Zhou, Y. Su, and E. Zhang, "Adaptive model-parameter-free fault-tolerant trajectory tracking control for autonomous underwater vehicles," *ISA Trans.*, vol. 114, pp. 57–71, Aug. 2021.
- [55] H. Jian, S. Zheng, P. Shi, Y. Xie, and H. Li, "Consensus for multiple random mechanical systems with applications on robot manipulator," *IEEE Trans. Ind. Electron.*, vol. 71, no. 1, pp. 846–856, Jan. 2024.
- [56] S. Wang, H. Zhang, S. Baldi, and R. Zhong, "Leaderless consensus of heterogeneous multiple Euler-Lagrange systems with unknown disturbance," *IEEE Trans. Autom. Control*, vol. 68, no. 4, pp. 2399–2406, Apr. 2023.
- [57] W. Zhao, Y. Liu, and X. Yao, "Adaptive fuzzy containment and vibration control for multiple flexible manipulators with model uncertainties," *IEEE Trans. Fuzzy Syst.*, vol. 31, no. 4, pp. 1315–1326, Apr. 2023.
- [58] M. Maadani and E. A. Butcher, "Pose consensus control of multi-agent rigid body systems with homogenous and heterogeneous communication delays," *Int. J. Robust Nonlinear Control*, vol. 32, no. 6, pp. 3714–3736, Apr. 2022.
- [59] S. A. Samy, Y. Cao, R. Ramachandran, J. Alzabut, M. Niezabitowski, and C. P. Lim, "Globally asymptotic stability and synchronization analysis of uncertain multi-agent systems with multiple time-varying delays and impulses," *Int. J. Robust Nonlinear Control*, vol. 32, no. 2, pp. 737–773, Jan. 2022.
- [60] X. M. Zhang, M. Wu, J. H. She, and Y. He, "Delay-dependent stabilization of linear systems with time-varying state and input delays," *Automatica*, vol. 41, no. 8, pp. 1405–1412, Aug. 2005.
- [61] A. Clark, "Control barrier functions for stochastic systems," *Automatica*, vol. 130, Aug. 2021, Art. no. 109688.
- [62] W. Xiao, C. Belta, and C. G. Cassandras, "Adaptive control barrier functions," *IEEE Trans. Autom. Control*, vol. 67, no. 5, pp. 2267–2281, May 2022.
- [63] W. Xiao, C. A. Belta, and C. G. Cassandras, "Sufficient conditions for feasibility of optimal control problems using control barrier functions," *Automatica*, vol. 135, Jan. 2022, Art. no. 109960.
- [64] W. S. Cortez, D. Oetomo, C. Manzie, and P. Choong, "Control barrier functions for mechanical systems: Theory and application to robotic grasping," *IEEE Trans. Control Syst. Technol.*, vol. 29, no. 2, pp. 530–545, Mar. 2021.
- [65] B. Gangopadhyay, P. Dasgupta, and S. Dey, "Safe and stable RL (S^2 RL) driving policies using control barrier and control Lyapunov functions," *IEEE Trans. Intell. Veh.*, vol. 8, no. 2, pp. 1889–1899, Feb. 2023.
- [66] H. K. Khalil, *Nonlinear Systems*, 3rd ed. Upper Saddle River, NJ, USA: Prentice-Hall, 2002.
- [67] N. Quan and K. Sreenath, "Exponential control barrier functions for enforcing high relative-degree safety-critical constraints," in *Proc. Amer. Control Conf.*, 2016, pp. 322–328.
- [68] W. Xiao and C. Belta, "Control barrier functions for systems with high relative degree," in *Proc. IEEE Conf. Decis. Control*, 2019, pp. 474–479.
- [69] F. Castaneda, J. J. Choi, B. Zhang, C. J. Tomlin, and K. Sreenath, "Pointwise feasibility of Gaussian process-based safety-critical control under model uncertainty," in *Proc. IEEE Conf. Decis. Control*, 2021, pp. 6762–6769.
- [70] C. I. G. Chinelato and B. A. Angelico, "Robust exponential control barrier functions for safety-critical control," in *Proc. Amer. Control Conf.*, 2021, pp. 2342–2347.
- [71] A. Greenbaum and T. Chartier, *Numerical Methods: Design, Analysis, and Computer Implementation of Algorithms*. William St. Princeton, NJ, USA: Princeton Univ. Press, 2012.
- [72] L. N. Trefethen, "Is Gauss quadrature better than Clenshaw-Curtis?," *SIAM Rev.*, vol. 50, no. 1, pp. 67–87, Mar. 2008.
- [73] L. Jiang, Z. Jin, and Z. Qin, "Distributed optimal formation for uncertain Euler-Lagrange systems with collision avoidance," *IEEE Trans. Circuits Syst. II, Exp. Briefs*, vol. 69, no. 8, pp. 3415–3419, Aug. 2022.



Zilong Song (Student Member, IEEE) received the B.E. degree in mechanical engineering from the Shandong University of Science and Technology, Qingdao, China, in 2022. He is currently working toward the master's degree in mechanical engineering with the Ocean College, Zhejiang University, Hangzhou, China. His research interests include multi-agent systems and safety-critical control.



Zheyuan Wu (Student Member, IEEE) received the B.E. and M.S. degrees in naval architecture and ocean engineering from Harbin Engineering University, Harbin, China, in 2018 and 2021, respectively. He is currently working toward the Ph.D. degree in ocean technology and engineering with Ocean College, Zhejiang University, Hangzhou, China. His research interests include AUV tracking control and multiple AUV systems control.



Haocai Huang (Member, IEEE) received the B.S. and M.S. degrees in mechanical engineering from Huaqiao University, Quanzhou, China, in 2001 and 2004, respectively, and the Ph.D. degree in mechanical engineering from Zhejiang University, Hangzhou, China, in 2010. He is currently a Professor with the Ocean College, Zhejiang University. His research interests include ocean engineering and autonomous underwater vehicles control theory.